Runaway Current Termination in JT-60U

H. Tamai 1), R. Yoshino 1), S. Tokuda 1), G. Kurita 1), Y. Neyatani 1), M. Bakhtiari 2),
R. R. Khayrutdinov 3), V .Lukash 4), M. N. Rosenbluth 5), and the JT-60 Team 1)

1) Japan Atomic Energy Research Institute, Naka-machi, Ibaraki-ken, 311-0193, Japan
2) Utsunomiya University, Utsunomiya, Tochigi, 321-8585, Japan
3) Troitsk Institute, 142092 Moscow, Russia
4) RRC Kurchatov Institute, 123182, Moscow, Russia
5) General Atomics, San Diego, California 92186-5698, USA

e-mail contact of main author: tamai@naka.jaeri.go.jp

Abstract. Spontaneous termination of runaway current, generated at the plasma disruption, is found in JT-60U during the vertical plasma displacement event, where the safety factor at the plasma surface, q_S decreases. For all shots with runaway electron generation, runaway current termination starts with the appearance of a spike in magnetic fluctuation and finishes at q_S 2. Growth rates of the spikes in the magnetic fluctuations decrease by an order of magnitude during the termination of runaway current. When each magnetic fluctuation with a slow growth rate appears, runaway current decays, and heat flux pulses are generated. Halo current during the runaway termination is small. Halo current is generated after the runaway termination, and reaches the maximum level at $q_S \sim 1$.

1. Introduction

In recent studies on major plasma disruption, the causality and the method for suppression are well understood. A proper control avoids or mitigates the disruption with relatively slow time scale after the precursor of the disruption is detected. In such a control, runaway electrons should be avoided and suppressed, since the runaway electrons reduce the life time of the first wall through the plasma wall interaction due to their intense energy and long confinement time. Therefore, the establishment of the method to avoid or to terminate runaway electrons, and the estimation of their influence on in-vessel component are urgent tasks for ITER. It has been reported that the runaway electrons surviving in the plasma of surface safety factor $q_S=1$, deposited the intense heat load [1].

On the other hand, in JT-60U the avoidance of runaway electrons generation at the plasma current quench has been found either when the magnetic perturbation was applied [2], or at the effective safety factor $q_{eff} < 2.5$ [3]. It was predicted that the confinement of runaway electrons was degraded by the breakdown of toroidal momentum conservation. In a recent simulation study [4] the relativistic electron motion has been analysed in the magnetic perturbation with toroidal asymmetry. The loss rate was enhanced with higher electron energy and with strong stochasticity of magnetic islands. Such aspects are desirable to reduce the influence of runaway electrons on the in-vessel component. Recently in JT-60U, the termination of runaway currents are achieved in the presence of low-n magnetic fluctuations around $q_S=3$, or $q_S=2$ [5].

In this paper, recent investigation of the termination process of runaway current, including the behaviour of magnetic fluctuation, and the measurement of the heat flux and the halo current at the runaway termination is presented.

2. Process of the runaway electron termination

In JT-60U spontaneous termination of generated runaway electrons has been investigated for the first time during the processes of (a) inward shift of plasma, (b) vertical shift of plasma, and (c) increase of the plasma current [5]. In those processes the surface or effective edge safety factor decreases to 3 or 2 at the fast termination of runaway electrons. Growth of the magnetic fluctuation with n=1 mode were always observed at the start of runaway current termination. These observations suggest that some MHD instabilities trigger the fast runaway current termination.

Figure 1 shows the temporal evolution of plasma parameters during the presence of runaway electron current. Plasma current, I_p, was decreased by the pre-programmed control. Current quench was caused at 2.757s, then the surface voltage, V_s, increased and the runaway electrons were generated, which was confirmed by hard X-ray emission, I_{HX}, with the energy larger than 1MeV. After the generation of runaway current, the plasma was controlled to shift downward as indicated by Z_j as shown in Fig.2 in order to simulate the vertical displacement event (VDE). The surface safety factor, q_s, decreased by the downward shift. The termination of runaway current started at t=2.94s at q_s~3 where a spike in hard X-ray coincided with the growth of the magnetic fluctuation. The surface voltage stayed at nearly zero until the start of the runaway current termination. Therefore, the plasma current was driven by runaway electrons before the termination. The termination of runaway current finished at q_s~2.5.

Figure 3 shows the q_s at the finish of runaway termination plotted against that at the start of runaway termination for the shots in which runaway electrons were generated. All the data points indicate that the termination of runaway current was finished at q_s 2.

3. Magnetic fluctuation

In all the shots in which the runaway current is generated, hard X-ray spike coincides with intense magnetic fluctuation which appears around a rational q_s or q_{eff} at the instance of the runaway termination. Figure 4 shows the temporal evolution of the surface safety factor, plasma current, and its time derivative, magnetic fluctuation with toroidal mode number of n=1, the growth rate of each spike in n=1 mode, and the poloidal mode number, m, during the runaway termination. Deposited power on the inner divertor plates and the hard X-ray emission are also shown, which are described and discussed in next section. Growth rate was deduced from e-folding time for each spike of the magnetic fluctuation. Poloidal mode number was deduced from the phase inverse in the signal of each poloidal channel of magnetic loop.

Many spikes in magnetic fluctuation appeared during the runaway termination. The first magnetic fluctuation is followed by repeated magnetic fluctuations. Current decayed during those repeated magnetic fluctuations appeared. Growth rate of the first spike was $3.3 \times 10^4 s^{-1}$. Growth rate of repeated magnetic fluctuations decreased during the runaway termination and slowed down to $5 \times 10^3 s^{-1}$. Poloidal mode number was changed from 3 to 2 during the runaway termination.

Magnetic fluctuations appeared at t=2.90-2.93s in Fig.1(f) were single spike. Each spike corresponded to the large spike in hard X-ray emission, and decreased the plasma current by a small amount. However, the runaway current was not terminated by such a spike.

Those measurements show that repeated magnetic fluctuations after the first magnetic fluctuation is necessary for the termination of runaway current.

4. Heat load on the first wall

Heat load on the first wall during the runaway current termination is also the large interest, since the fast termination of runaway electrons associates with the frequent large spikes in hard X-ray which consequently may cause the heat load on the first wall. Therefore, the heat load deposited on the first wall during the runaway termination was estimated by the measurement of the divertor heat flux. Heat flux at the divertor plates and private dome were measured by infrared TV-camera (IRTV) with a sampling rate of 4kHz.

Figure 5 shows the viewing area of IRTV to measure the heat flux on the divertor plates and private dome, and the measured profile of heat flux at 2.9365s and at 2.9397s when the peak of heat flux were measured during the runaway current termination. Heat flux only at the inner divertor plates was detected since the plasma touched outside plates out of the viewing area of IRTV. Heat load was estimated from the measured heat flux at the inside plates. In Fig.4(f) the temporal evolution of deposited power on the inside divertor plates is shown. Deposited power during the current decay was intensive pulses with the duration of the order of hundred micro seconds as indicated by the shade, and did not deposit as constant heat load during the current decay.

Spikes in hard X-ray emission, shown in Fig.4(g) corresponds to the spikes in the deposited power and are considered to arise the wall interaction with the runaway electrons. Two peaks in the deposited power coincided to the magnetic fluctuation of $n=1$ with the slow growth rate rather than fast one. Two peaks in the deposited power also coincided to the peaks in the current decay rate, $-dIp/dt$, followed by the drop of current decay rate, which may suggest the redistribution of plasma current.

5. Halo current

With a fast movement of plasma position in reducing the surface safety factor, halo current is often generated on the in-vessel components at the plasma current termination. Previous analytic model of halo current has shown that the peak halo current can be low at high surface q [6]. Furthermore, a halo current spike has been observed at $q_S \sim 1$ in JT-60U [7]. It is quite important to clarify the generation of halo current related to the process of runaway electron termination.

Figure 6 shows the temporal evolution of plasma current, hard X-ray emission, calculated toroidal halo current, surface safety factor, measured and calculated halo current at the termination of runaway electron current. Measurement of halo current was done by Rogowski coil installed under the baffle plates, and averaged toroidally. Calculation of halo current was done by the plasma equilibrium analysis using with DINA-code, in which the eddy current along the vacuum vessel is taken into account [8]. Calculated result agrees well with measured one both in the temporal behaviour and in the absolute value. At the finish of the runaway current termination (t=2.94s), halo current was low level. Halo current increased after the termination of runaway current, and reached its maximum at $q_S \sim 1$, where the surface safety factor is defined at the boundary of core plasma. Figure 7 shows the temporal evolution of the poloidal equilibrium cross section deduced from DINA-code analysis. Halo region, indicated by the solid lines, does not exist at $q_S > 2$, while appears at $q_S < 2$ and grows to almost full plasma region at maximum halo current (t=2.965s).

In Fig.8 the intensity of hard X-ray emission is plotted against the measured halo current for 4 disruption shots in which the runaway current was generated. Plots are distinguished by the surface safety factor, q_S. Solid, and open circles show the cases for $q_S > 2$, and those for $q_S < 2$.

It is clearly confirmed in the figure that the halo current level is small at $q_S > 2$, and increases at $q_S < 2$ in the disruption shots with runaway current generation.

In Fig.9 the toroidal distribution of measured halo current is shown. The temporal evolution in every 0.25ms is plotted. The distribution did not change with time and the halo current had the toroidal asymmetry of n=1, which is the same as that previously observed in vertical displacement event without the generation of runaway electrons [9]

6. Conclusions

Runaway current was terminated at simulated VDE by controlled plasma shift in JT-60U. Termination of runaway electron current at the safety factor q_S 2 was established. Magnetic fluctuation, heat load and halo current were measured during the termination. Those observations are summarised as follows:

(1) The termination of runaway current starts with the appearance of a large spike in magnetic fluctuation with the toroidal mode number n=1, and finishes at q_S 2.

(2) The first magnetic fluctuation with a fast growth rate of an order of $10^4 s^{-1}$ is followed by repeated magnetic fluctuations with slow growth rates of an order of $10^3 s^{-1}$. Those fluctuations decay the current and terminate the runaway current.

(3) Heat flux pulses on the divertor plates during the runaway termination are observed with the duration of the order of hundreds micro seconds. The heat pulses correspond to the appearance of magnetic fluctuations with slow growth rates, which causes the increase of current decay rate.

(4) Halo current is very small during the runaway termination, and then it increases at $q_S < 2$.

References

[1] Putvinski, S., *et al.*, 17th IAEA Conf., Yokohama (1998) ITERP1/10.
[2] Kawano, Y., *et al.*, 24th EPS Conf. Berchtesgaden, **21A**, Part II (1997) 501.
[3] Yoshino, R., *et al.*, Nucl. Fusion **39** (1999) 151.
[4] Tokuda, S., *et al.*, Nucl. Fusion **39** (1999) 1123.
[5] Yoshino, R., *et al.*, Nucl. Fusion **40** (2000) 1293.
[6] Humphreys, D.A., *et al.*, Phys. of Plasmas **6** (1999) 303.
[7] Neyatani, Y., *et al.*, Nucl. Fusion **39** (1999) 559.
[8] Khayrutdinov R.R., *et al.*, J. Comp. Physics, **109** (1993) 193.
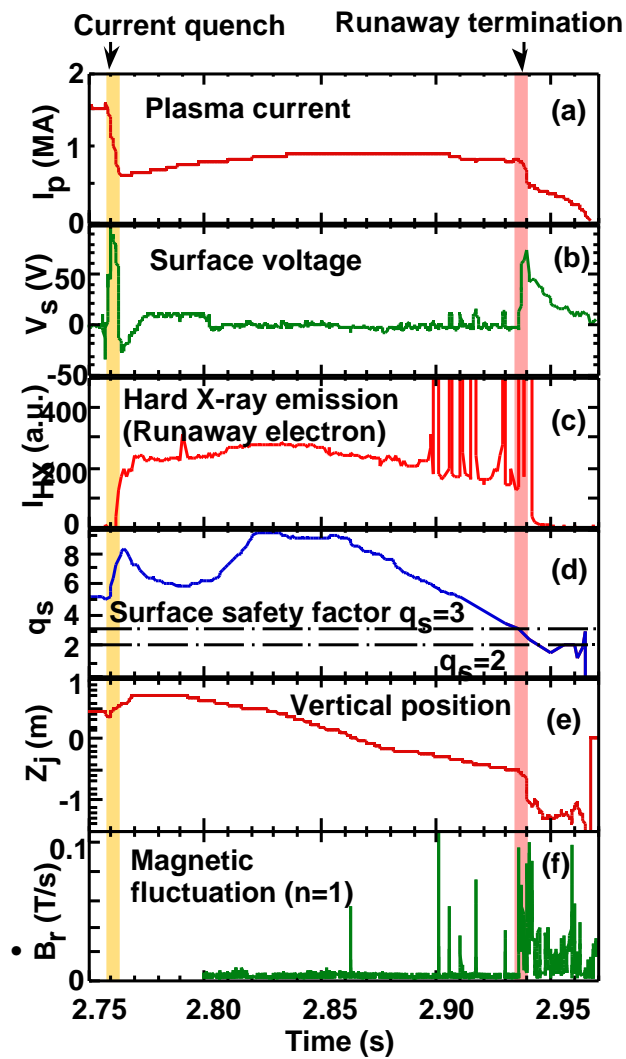[9] Neyatani, Y., *et al.*, 17th IAEA Conf., Yokohama (1998) EXP3/11.

Fig. 1 Temporal evolution of (a) plasma current, (b) surface voltage, (c) hard X-ray emission, (d) surface safety factor, (e) vertical plasma position, and (f) magnetic fluctuation of n=1.
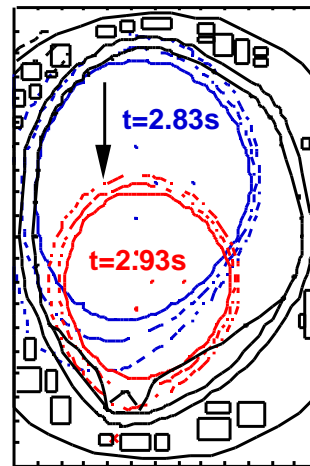

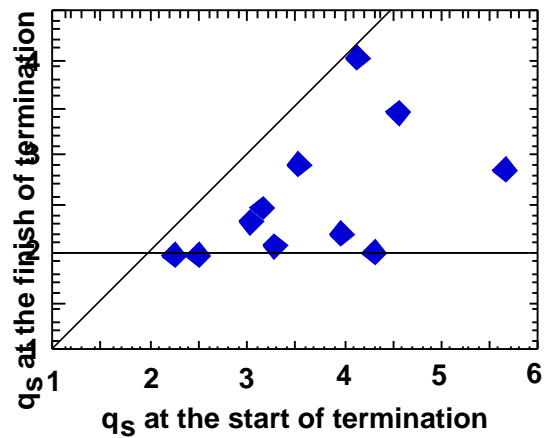Fig.2 Downward shift of plasma during runaway current phase.

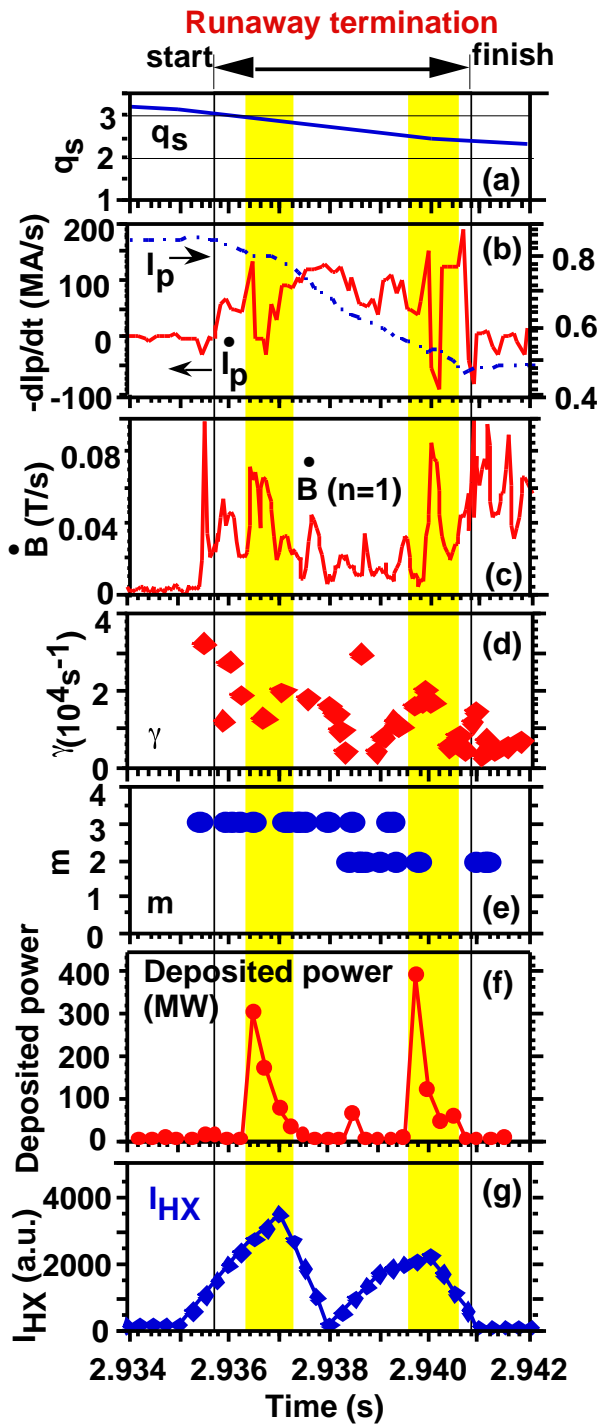Fig.3 Surface safety factor at the finish of runaway termination versus that at the start of runway termination.

Fig. 4 Temporal evolution of (a) the surface safety factor, (b) plasma current, and its decay rate, (c) magnetic fluctuation with toroidal mode number, n=1, (d) the growth rate of each spike in n=1 mode, (e) the poloidal mode number, m, (f) deposited power on the inside divertor plates, and (g) hard X-ray emission, during the runaway termination.
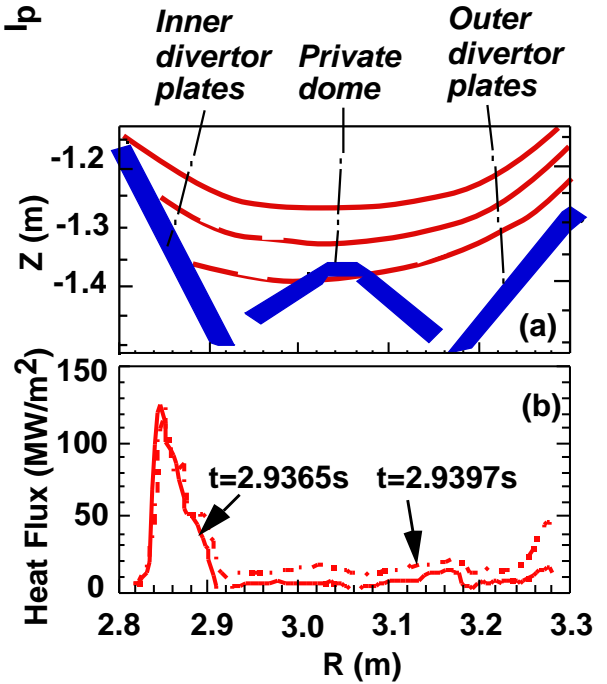

Fig. 5 (a) Viewing area of IRTV , and (b) profile of heat flux at t=2.9365s (solid line) and at t= 2.9397s (dotted line) when the peak of heat flux were measured during the runaway current termination.
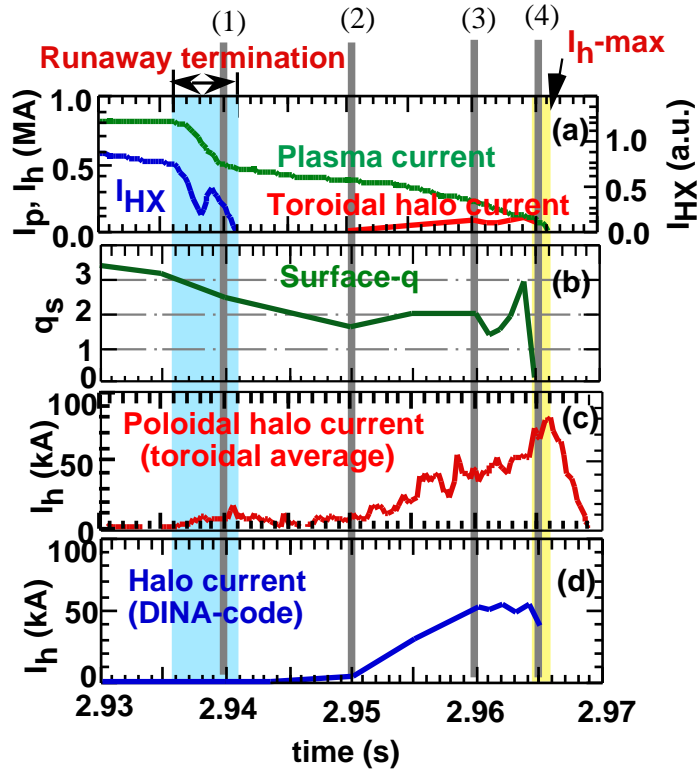
Fig.6 Temporal evolution of (a) plasma current, runaway electrons (Hard X-ray emission), toroidal halo current, (b) surface safety factor, (c) poloidal halo current by Rogowski coil measurement, and (d) that by DINA-code analysis, during and after the termination of runaway current. Toroidal halo current is deduced by DINA-code analysis.
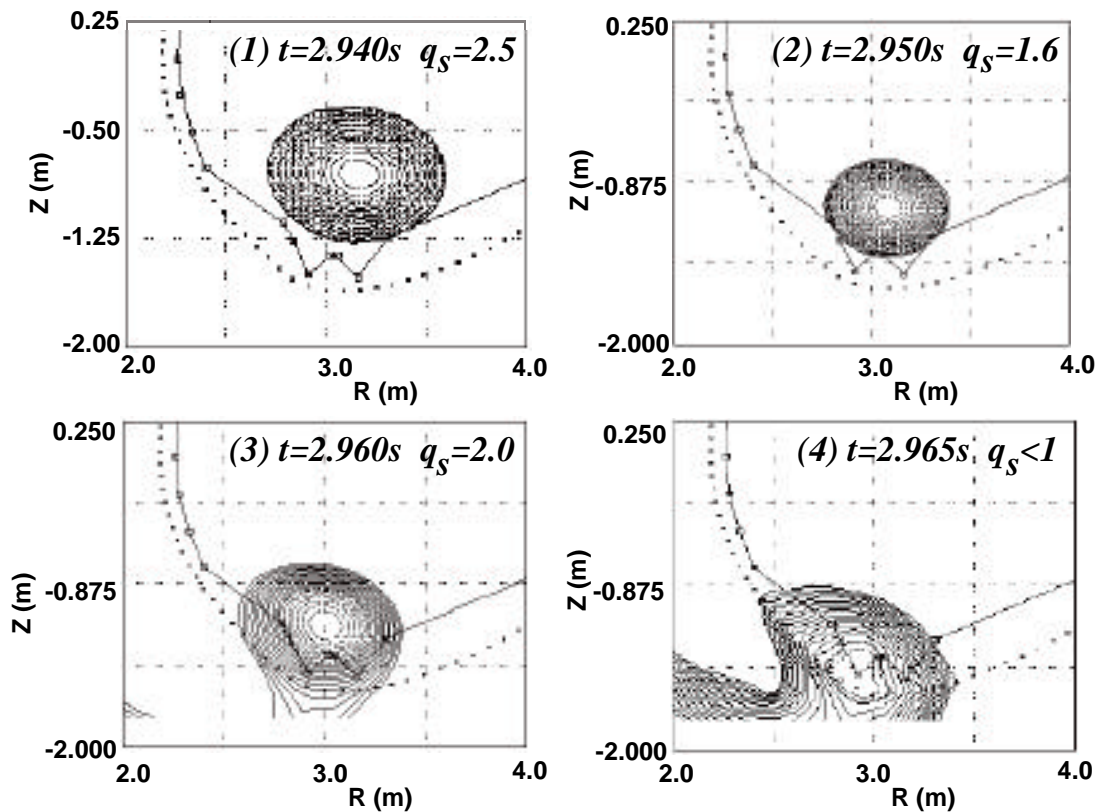

Fig.7 Temporal evolution of poloidal equilibrium cross section analysed by DINA-code. Solid lines indicate the halo region.
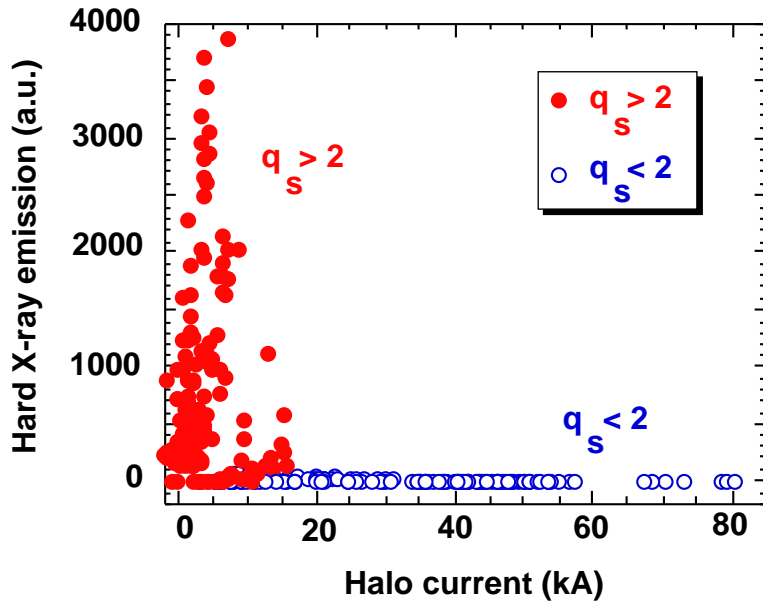
Fig.8 Intensity of hard X-ray emission plotted against
the measured halo current for 4 disruption shots in
which the runaway current was generated. Solid and
open circles indicate the surface safety factor, $q_S>2$,
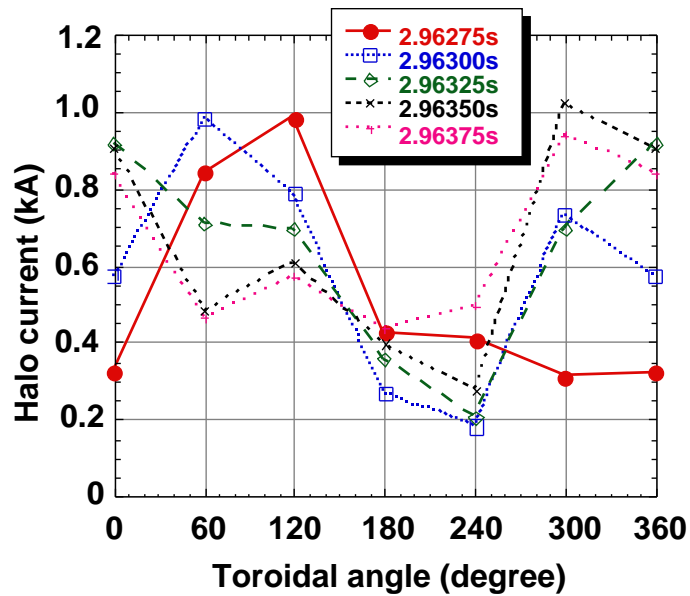and $q_S<2$, respectively.

Fig.9 Toroidal distribution of measured halo current
with the temporal evolution in every 0.25ms during
increase phase of halo current (2.96275s-2.96475s).